BIOCHEMISTRY
including biophysical chemistry & molecular biology

Article

pubs.acs.org/biochemistry

Role of Phospholipids of Subunit III in the Regulation of Structural Rearrangements in Cytochrome *c* Oxidase of *Rhodobacter sphaeroides*

Khadijeh S. Alnajjar,[†] Teresa Cvetkov,[‡] and Lawrence Prochaska*

Department of Biochemistry and Molecular Biology, Boonshoft School of Medicine at Wright State University, Dayton, Ohio 45435, United States

ABSTRACT: Subunit III of cytochrome *c* oxidase possesses structural domains that contain conserved phospholipid binding sites. Mutations within these domains induce a loss of phospholipid binding, coinciding with decreased electron transfer activity. Functional and structural roles for phospholipids in the enzyme from *Rhodobacter sphaeroides* have been investigated. Upon the removal of intrinsic lipids using phospholipase A_2, electron transfer activity was decreased 30−50%. Moreover, the delipidated enzyme exhibited turnover-induced, suicide inactivation, which was reversed by the addition of exogenous lipids, most specifically by cardiolipin. Cardiolipin exhibited two sites of interaction with the delipidated enzyme, a high-affinity site (K_m = 0.14 μM) and a low-affinity site (K_m = 26 μM). Subunit I of the delipidated enzyme exhibited a faster digestion rate when it was treated with α-chymotrypsin compared to that of the wild-type enzyme, suggesting that lipid removal induces a conformational change to expose the digestion sites further. Upon reaction of subunit III of the enzyme with a fluorophore (AEDANS), fluorescence anisotropy showed an increased rotational rate of the fluorophore in the absence of lipids, indicating increased flexibility of subunit III within the enzyme's tertiary structure. Additionally, Förster resonance energy transfer between AEDANS and a fluorescently labeled cardiolipin revealed that cardiolipin binds in the v-shaped cleft of subunit III in the delipidated enzyme and that it moves closer to the active site in subunit I upon a change in the redox state of the enzyme. In conclusion, these results show that the phospholipids regulate events occurring during electron transfer activity by maintaining the structural integrity of the enzyme at the active site.

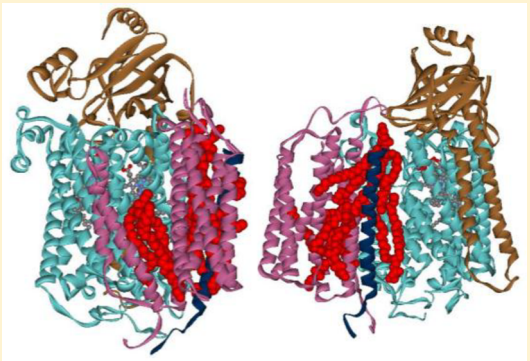

Cytochrome *c* oxidase (COX) is a component of the electron transport chain located in the mitochondrial inner membrane, which catalyzes the reduction of molecular oxygen to produce two water molecules while pumping one proton per electron transferred.[1] The catalytic core of COX is composed of three subunits that are highly conserved across species; they contain the redox centers and are required for efficient activity.[2] Subunit I (SUI) of COX contains heme *a* and the binuclear center, composed of heme a_3 and Cu_B. Additionally, SUI contains two proton translocation pathways, the K- and D-channels, named after essential amino acids within the channels, K362 and D132,[a] respectively (*Rhodobacter sphaeroides* numbering).[3] Two of the substrate protons (used to reduce oxygen) are transferred through the K-channel, while the other two substrate protons, in addition to all pumped protons, are transferred through the D-channel.[3] Subunit II (SUII) contains the cytochrome *c* binding domain and a diatomic-copper center (Cu_A). Subunit III (SUIII) is highly hydrophobic and does not contain metal centers. Several studies suggested a possible role of this subunit in maintaining the structural integrity and rapid turnover rate through regulation of proton uptake, oxygen delivery, and proton exit;[4−9] however, the exact function has yet to be determined.

SUIII is located adjacent to SUI in the three-dimensional structure of COX.[3] It contains seven transmembrane α-helices that are arranged to form a v-shaped cleft with helices 1 and 2 as one bundle and helices 3−7 as the second bundle. The three-dimensional structure of SUIII from *R. sphaeroides* (*RBS*) contains six bound phospholipids, identified as phosphatidylethanolamine (PE), which interact with the enzyme at different locations.[3] SUIII contains conserved phospholipid binding sites within the cleft, where two PEs are intercalated within helices 2, 3, and 6 of SUIII.[3] The other four phospholipids are positioned at the interface between SUI, SUIII, and SUIV. The phosphate headgroups of the phospholipids in the v-shaped cleft of SUIII form electrostatic interactions with R137 (SUI) and R226 (SUIII), and the fatty acid chains form van der Waals interactions with W58 and W59 as well as with other conserved residues in SUIII.[10]

These lipids have been shown to be important in catalytic activity.[10−12] The removal of the phospholipids weakens the interactions between SUI and SUIII, leading to the loss of SUIII.[10] Additionally, the enzyme undergoes turnover-induced,

Received: November 3, 2014
Revised: December 31, 2014
Published: January 5, 2015

DOI: 10.1021/bi5013657
Biochemistry 2015, 54, 1053−1063

suicide inactivation in the absence of the lipids, which leads to an alteration in the integrity of the active site and the ultimate loss of Cu_B. However, rates of uptake of protons through the D- and K-channels in SUI are unaffected by the removal of those lipids.[10] This suggests that SUIII contributes to efficient COX activity via long-range interactions, which also stabilize the structure of the enzyme. Thus, it was proposed that these lipids control the dynamic motion of the enzyme near the active site and that their absence causes increased flexibility at the active site, which consequently results in suicide inactivation.[13]

Cardiolipin (CL) has been shown to be important for the activity of COX isolated from bovine heart mitochondria.[12] The crystal structure of bovine heart COX shows two tightly bound CLs surrounding the catalytic core.[14] Upon the removal of these tightly bound CLs in bovine COX, steady-state activity decreases and some accessory subunits dissociate.[12] The addition of CL to delipidated COX induced a recovery of activity to WT COX, which was not observed with phosphatidylcholine (PC) or PE.[12] It has also been shown that the removal of tightly bound CL results in the loss of the low-affinity site of interaction of cytochrome *c* with COX.[11] It was proposed that the negatively charged CL aids in the docking of cytochrome *c* to COX by forming additional electrostatic interactions, which govern the interaction between the binding partners.[15] In support of this hypothesis, CL has been shown to be important in the activity of mitochondrial cytochrome bc_1.[16,17,18]

To test the role of phospholipids in the structural regulation of *RBS* COX, phospholipase A_2 was used to remove the lipids. Results show that the delipidated COX exhibits biphasic kinetics in the presence of CL and that the low-affinity cytochrome *c* site for interaction is lost in the absence of phospholipids. Additionally, Förster resonance energy transfer (FRET) studies between fluorescently labeled SUIII and a fluorescently labeled CL show that the phospholipids modulate the dynamic motion of COX during redox events.

MATERIALS AND METHODS

Expression and Purification of Cytochrome *c* Oxidase. *R. sphaeroides* cells were grown as previously reported by Zhen et al.[19] WT COX was purified from the *n*-dodecyl β-D-maltoside (DM)-solubilized membranes using affinity chromatography on a Ni^{2+}-NTA column. The enzyme was eluted from the column with 100 mM histidine, washed, and concentrated by ultrafiltration using 10 mM Tris-HCl (pH 8.0), 40 mM KCl, and 0.1% DM using Millipore YM-100 filters. The concentration was determined spectrophotometrically (reduced − oxidized $\Delta\varepsilon_{606-630}$ = 28.9 mM^{-1} cm^{-1}).[20] SUIII-depleted COX (I-II oxidase) was prepared by incubation in 12% Triton X-100 for 30 min at 4 °C. The mixture was loaded onto a Ni-NTA column, washed with 10 mM Tris-HCl (pH 8.0), 40 mM KCl, and 0.1% DM, and eluted with 100 mM histidine.[21]

Removal of Phospholipids. WT COX was incubated with equimolar amounts of phospholipase A_2 (PLA_2) (from honey bee venom provided by Sigma-Aldrich, 600−2400 units/mg of protein) in 20 mM MOPS (pH 7.2), 10 mM $CaCl_2$, and 10% glycerol, in the presence of 1 mg of DM/mg of COX. The reaction continued for 3 h at 4 °C and was quenched with 50 mM EDTA.[22] The delipidated enzyme was diluted with 5 mM potassium phosphate (pH 8.0) and 0.1% DM, loaded onto a cytochrome *c* affinity column, eluted with 5 mM potassium phosphate (pH 8.0), 0.1% DM, and 50 mM NaCl, and concentrated with Millipore YM-100 filters.[23]

Measurement of Phospholipid Content. Purified COX samples were incubated with 10 mM EDTA for 15 min and then washed three times in Millipore YM-100 filters with 10 mM Tris-HCl (pH 7.4) and 40 mM KCl prepared in metal-free water. Sixty-five micrograms of COX was diluted with 3 mL of metal-free water. Standards of iron, copper, and phosphorus were prepared at concentrations ranging from 0 to 75 μg/L. Samples were analyzed using an Elan 9000 inductively coupled plasma mass spectrometer (ICP-MS), and the concentrations were intrapolated using a standard curve. Phosphorus was used to measure the phospholipid content in the sample. Iron and copper from COX preparations were used as internal standards, and data were normalized to 3 mol of copper/mol of COX.

Limited Proteolysis. COX was incubated with TLCK-treated α-chymotrypsin (Worthington) at a 10:1 (w/w) COX:chymotrypsin ratio in 20 mM Tris-HCl (pH 8.0) at 25 °C for up to 5 h and the reaction stopped using 1 mM PMSF. The digested enzyme was incubated with 2% SDS at 37 °C for 30 min and then run on a SDS−urea polyacrylamide gel.[24] Gels were stained with Coomassie Blue and viewed using a Fuji LAS-3000 Imager. The staining intensity of SUI was measured using Multi Gauge and plotted as a function of digestion time.

Recovery of Oxygen Reduction Activity. Oxygen reduction activity was measured polarographically in 50 mM potassium phosphate (pH 7.4) and 0.1% DM in the presence of 17 mM ascorbic acid, 0.6 mM TMPD, and 20 μM cytochrome *c* at 25 °C. Lipids were solubilized in assay buffer by sonication to clarity at 4 °C. COX (2 μM) was incubated with each lipid ligand for at least 15 min prior to the assay.

Steady-State Cytochrome *c* Kinetics. The cytochrome *c* concentration dependence of COX electron transfer activity was measured polarographically in 25 mM Tris-acetate (pH 7.8) and 0.1% DM in the presence of 17 mM ascorbic acid and 0.6 mM TMPD at 25 °C.[25] Cytochrome *c* was varied in concentration from 0.1 to 10 μM. The enzyme was preincubated with 500 μM CL where indicated.

Labeling with IAEDANS. COX was incubated with IAEDANS at a 10:1 IAEDANS:COX molar ratio in 20 mM HEPES (pH 8.0) and 0.1% DM at 25 °C and in the dark for 1 h.[26] The reaction was quenched with a 100-fold molar excess of dithiothreitol and the mixture washed a minimum of three times with 20 mM HEPES (pH 8.0) using Millipore YM-100 filters. Potassium ferricyanide was used to oxidize the enzyme. The AEDANS:COX binding stoichiometry was determined using the absorbance at 336 nm (ε_{336} = 5.7 mM^{-1} for AEDANS)[27] in a Hewlett-Packard 2451 diode array spectrophotometer and corrected for the absorbance of oxidized COX at 336 nm (ε_{336} = 44 mM^{-1} for COX). SDS−PAGE was used to test the specificity of labeling to SUIII, and AEDANS fluorescence was monitored (excitation at 312 nm) using a Fuji LAS-3000 Imager.[24] Gels were subsequently stained with Coomassie Blue.

Förster Resonance Energy Transfer (FRET). TopFluor-labeled cardiolipin (TFCL) {1,1′,2,2′-tetraoleoyl cardiolipin [4-(dipyrromethaneboron difluoride) butanoyl] (ammonium salt)} (Avanti Polar Lipids) was solubilized in 50 mM potassium phosphate (pH 7.4) and 50 μM DM. FRET from AEDANS-labeled COX (donor; λ_{ex} = 336 nm, and λ_{em} = 470 nm) to TFCL (acceptor; λ_{ex} = 490 nm, and λ_{em} = 505 nm) was measured using an ISS PC1 spectrofluorimeter with 1 mm slits. TFCL (1 μM) was added to 0.5 μM AEDANS-labeled COX in 50 mM potassium phosphate (pH 7.4) and 50 μM DM, and energy transfer was monitored as a function of time. FRET was

DOI: 10.1021/bi5013657
Biochemistry 2015, 54, 1053−1063

measured with the oxidized enzyme and in the presence of 0–40 mM ascorbic acid. For distance measurements, the refractive index was assumed to be 1.43 in a solution of 0.1% DM,[28] and the fluorescence quantum yield of the donor in the absence of the acceptor is reported to be 0.94.[29] Additionally, the dipole angular orientation factor was assumed to be at $^2/_3$ for dynamic motion of the donor and the acceptor.[30] These assumptions were used to calculate the Förster distance of 53.1 ± 0.4 Å. The efficiency of energy transfer was calculated using the quenching of AEDANS emission by TFCL and corrected for the inner filter effect resulting from the absorbance of COX and ascorbic acid.[31]

For all the reported results, experiments were performed a minimum of three times, and the averages with standard deviations are reported.

RESULTS

The removal of endogenous lipids from *RBS* COX results in reduced steady-state activity and in suicide inactivation.[10,11] These events indicate that lipids play an important role in the regulation of structural flexibility at the active site of SUI, which in turn modulates steady-state activity. Thus, this study is aimed to clarify the role of phospholipids in the structure and function of COX.

Removal of the Phospholipids from *RBS* COX. WT COX was treated with molar stoichiometric amounts of PLA_2 in the presence of DM to remove the phospholipids embedded in the enzyme without inducing major perturbations in SUI–SUIII interactions.[12,18,21] Loss of phospholipids because of the treatment was confirmed by ICP-MS as the ratio of phosphorus per mole of COX (Table 1). Iron and copper (from COX) were used as internal standards, and phosphorus was quantified relative to 3 mol of copper. Table 1 shows that purified WT COX retained 5–6 mol of phosphorus as phospholipids/mol of COX. Upon treatment with PLA_2, the enzyme lost most of its phospholipid content (<1 mol of P/mol of COX) (Table 1). Additionally, I-II oxidase prepared by biochemical methods contained little or no phospholipid bound to COX in the absence of SUIII. This suggests that SUIII is necessary for the retention of phospholipids. COX isolated from bovine heart mitochondria was used as an additional control, which contains 17 phospholipids/mol of COX (5–8% phospholipid content by weight), similar to values published previously.[32]

The PLA_2-treated enzyme retained SUIII as confirmed by two-dimensional gel electrophoresis (Figure 1). The most intense band in the first dimension on the native gel (Figure 1A) contained enzyme with all subunits (Figure 1B), while the faster-running band contains I-II oxidase. Both the WT and delipidated enzyme contained approximately 10–15% I-II oxidase. Both the visible absorbance and the circular dichroism spectra of the hemes were unperturbed by delipidation. Additionally, the binding affinities of active site ligands such as azide, cyanide, and formate were unchanged by delipidation (data not shown).

Table 1. Physical Characterization of WT and Delipidated COX

	WT COX	delipidated COX
electron transfer activity (s^{-1})[a]	1300 ± 23	860 ± 6
suicide inactivation (CC_{50})[b]	3×10^{8}[c]	48000 ± 3000
phosphorus content[d]	5–6	<1

[a]As measured polarographically as described in Materials and Methods. [b]CC_{50} defined as the number of catalytic cycles the enzyme undergoes when 50% is inactivated. [c]As reported by Bratton et al.[21] [d]Measured by ICP-MS and reported as moles of phosphorus per 3 mol of copper. I-II oxidase contained <1 phosphorus, and bovine heart mitochondrial COX contained 17.

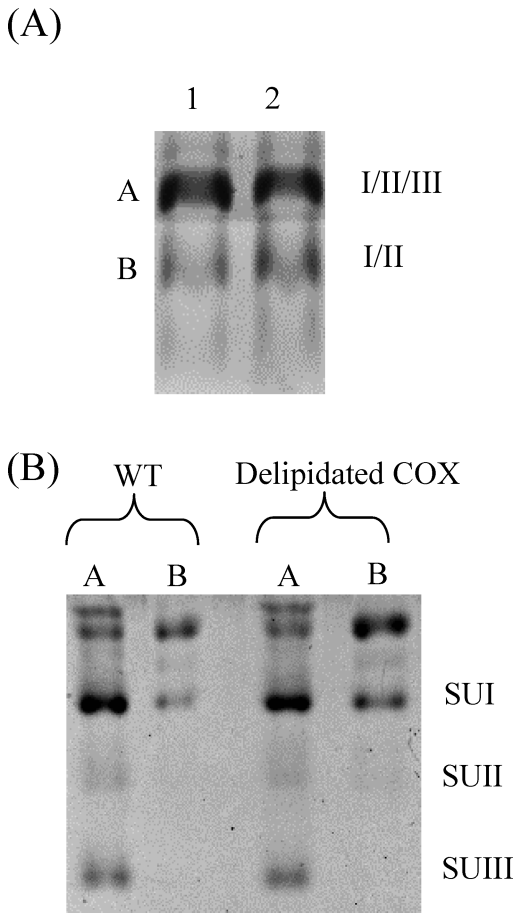

Figure 1. Gel electrophoresis of WT and delipidated COX. (A) Native gel electrophoresis: lane 1 (WT COX), nand A, intact complex, and band B, I-II oxidase (10% of the total preparation); lane 2 (delipidated COX), band A, intact complex, and band B, I-II oxidase (15% of total preparation). (B) Second-dimension SDS–PAGE of bands A and B of WT and delipidated COX. Serva Blue stain from the native gel was used to visualize bands under visible light using a Fuji LAS-3000 Imager. SUII is lightly stained because of the low detection limits of Serva Blue stain.

Upon delipidation, electron transfer activity of the enzyme was inhibited by 30–50% (Table 1). Activity of the delipidated enzyme was reconstituted to WT by the addition of asolectin (Table 2). Also, the delipidated enzyme exhibited suicide inactivation as measured in terms of CC_{50}, which recovered to the same value exhibited by WT COX upon the addition of asolectin.

Specificity of Activity Recovery to Exogenous Lipid Ligands. Soybean asolectin contains mostly PC and PE, in addition to phosphatidylglycerol (PG), phosphatidylserine, phosphatidic acid, and CL.[33] To specify which phospholipids in asolectin induced the recovery of activity in the delipidated enzyme to WT activity, experiments were conducted using individual purified phospholipids and combinations of the purified lipids.

DOI: 10.1021/bi5013657
Biochemistry 2015, 54, 1053–1063

Table 2. Summary of Activity Recovery in the Presence of Different Lipid Ligands in WT and Delipidated COX

ligand[a]	WT COX[b]	delipidated COX[b]
asolectin (soybean)	1.2 ± 0.08	1.5 ± 0.16[c]
CL (18:1)	1.1 ± 0.07	1.6 ± 0.01[c]
CL (from bovine heart; mostly 18:1, 18:2)	1.1 ± 0.07	2.2 ± 0.1[c]
arachidonic acid (20:4)	1.04 ± 0.05	1.9 ± 0.05[c]
oleic acid (18:1)	1.08 ± 0.09	1.9 ± 0.08[c]
stearic acid (18:0)	1.02 ± 0.1	1.9 ± 0.08[c]
lyso PC (bovine heart; mostly 16:0, 18:0, 18:1)	0.84 ± 0.03	0.96 ± 0.2[d]
PA (egg yolk; mostly 16:0, 18:0, 18:1, 18:2)	1.09 ± 0.07	1.16 ± 0.03[d]
PC (18:1)	1.07 ± 0.1	1.04 ± 0.1[d]
PE (18:1)	1.1 ± 0.14	0.96 ± 0.11[d]
PG (18:1)	1.27 ± 0.04	0.93 ± 0.06[d]
lauric acid (12:0)	0.89 ± 0.07	0.95 ± 0.04[d]

[a]Both WT and delipidated COX were incubated with each of those lipids at 500 μM for 15 min prior to the assay. [b]Values reported as fold activity increase resulting from incubation with different ligands as compared to that of the untreated control. [c]Statistically significant with $P < 0.001$ as compared to untreated delipidated COX. [d]Not statistically significant.

RBS membranes contain PE (40%), PG (22%), PC (20%), CL (6%), and other lipids.[34] In addition, the acyl chains of phospholipids are mainly composed of 18:1.[35,36] Thus, the stimulation of activity in the presence of these purified lipids was investigated. Table 2 shows that all the diacyl and monoacyl glycerides were ineffective in restoring activity. This was independent of the headgroup charge [PC (zwitterionic), PG (negative), phosphatidic acid (negative), and PE (zwitterionic)], acyl chain length (16:0 and 18:0), saturation (18:0, 18:1, and 18:2), and source (egg yolk and bovine heart). A combination of the different purified phospholipids also proved to be ineffective in restoring activity [PG and PE, PG and PC, PC and PE, and PC, PG, and PE (data not shown)]. Alternatively, incubating the enzyme with free long chain fatty acids (≥18C) stimulated a 2-fold increase in activity independent of chain length and saturation (18:0, 18:1, and 20:4). Most interestingly, the addition of CL stimulated the activity significantly. Though it has been shown previously that COX purified from bovine heart requires CL for full functional activity, there are no reports that describe the effect of CL on *RBS* COX[11,12,37] (see Discussion).

Figure 2 shows the dependence of the WT and delipidated COX activity on CL concentration. The WT activity is unaffected by the addition of CL. The delipidated enzyme exhibits two-site saturation kinetics, a high-affinity site with an apparent K_m value of 0.14 ± 0.01 μM and another with a low affinity of 26 ± 2.5 μM. The presence of two sites is consistent with similar observations in bovine heart COX.[12,38]

Delipidation Induces a Loss of the Low-Affinity Steady-State Kinetic Site of Interaction of Cytochrome *c* with COX. It has previously been reported that cytochrome *c* exhibits biphasic steady-state kinetics with WT COX.[25,39,40] Thus, the dependence of electron transfer activity on cytochrome *c* concentration was measured in the presence and absence of endogenous phospholipids (Figure 3). WT COX exhibits biphasic kinetics with apparent K_m values similar to those previously reported.[25] Delipidated COX exhibits a loss of the low-affinity site, confirming that the lipids are necessary for interaction of cytochrome *c* with COX. Upon incubation of the delipidated enzyme with CL, the biphasic kinetics is recovered with apparent K_m values similar to those of WT (Figure 3).

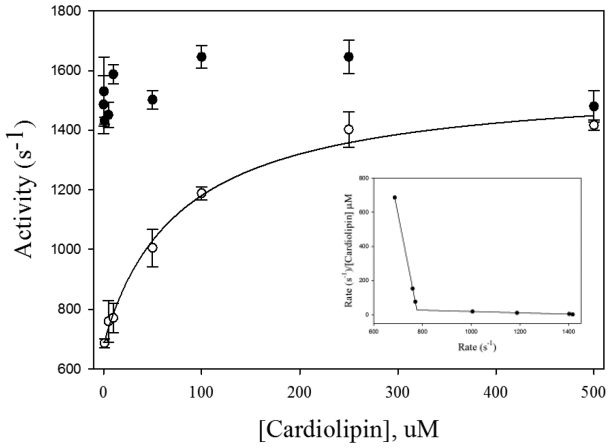

Figure 2. Effect of cardiolipin concentration on steady-state electron transfer activity in WT and delipidated COX. Measurements were taken in 50 mM potassium phosphate (pH 7.4) and 0.1% DM with either WT (●) or delipidated (○) COX. COX was incubated with CL at each of the reported concentrations for 15 min prior to the assay. Points were best fit with a saturation curve with two binding sites using Sigma Plot to obtain apparent K_m values of 0.14 ± 0.001 and 26 ± 2.5 μM for delipidated COX. The Eadie–Hofstee plot is shown in the inset for delipidated COX to show the two sites.

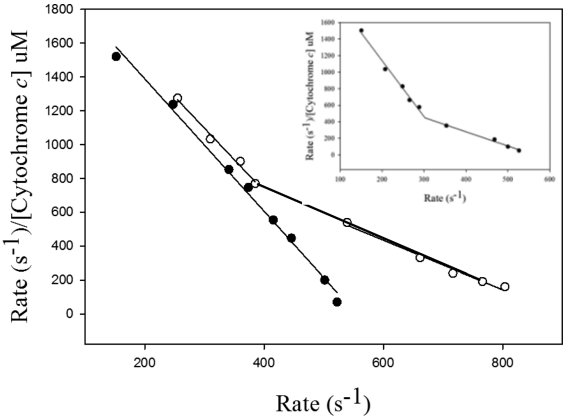

Figure 3. Steady-state kinetics of interaction of cytochrome *c* with WT and delipidated COX. Activity was measured polarographically at 25 °C in 25 mM Tris-acetate (pH 7.8) and 0.1% DM in the presence of 17 mM ascorbic acid, 0.6 mM TMPD, and various concentrations of cytochrome *c* (0.1–10 μM). Delipidated COX (●) exhibited an apparent K_m value of 0.26 ± 0.008 μM and a V_{max} of 552 ± 21 s^{-1}, while delipidated COX incubated in 500 μM CL (○) showed an apparent K_{m1} value of 0.26 ± 0.02 μM and a V_{max1} of 594 ± 53 s^{-1}, and an apparent K_{m2} value of 0.69 ± 0.05 μM and a V_{max2} of 928 ± 87 s^{-1}. WT data are shown in the inset (apparent K_{m1} value of 0.15 ± 0.01 μM and V_{max1} of 360 ± 30 s^{-1}, and apparent K_{m2} value of 0.58 ± 0.04 μM and V_{max2} of 550 ± 64 s^{-1}).

Increase in the Flexibility of SUI and SUIII upon Removal of Phospholipids. Delipidated COX has been shown to undergo irreversible suicide inactivation, suggesting that lipids are important in the structural integrity of the enzyme. To test this hypothesis, the time dependence of chymotrypsin digestion of SUI was monitored in WT and delipidated COX. Our previous work has shown that

DOI: 10.1021/bi5013657
Biochemistry 2015, 54, 1053–1063

chymotrypsin digestion of WT COX results in complete digestion of SUII and cleavage of SUI into two large fragments.[41] Figure 4 shows that the staining intensity of SUI

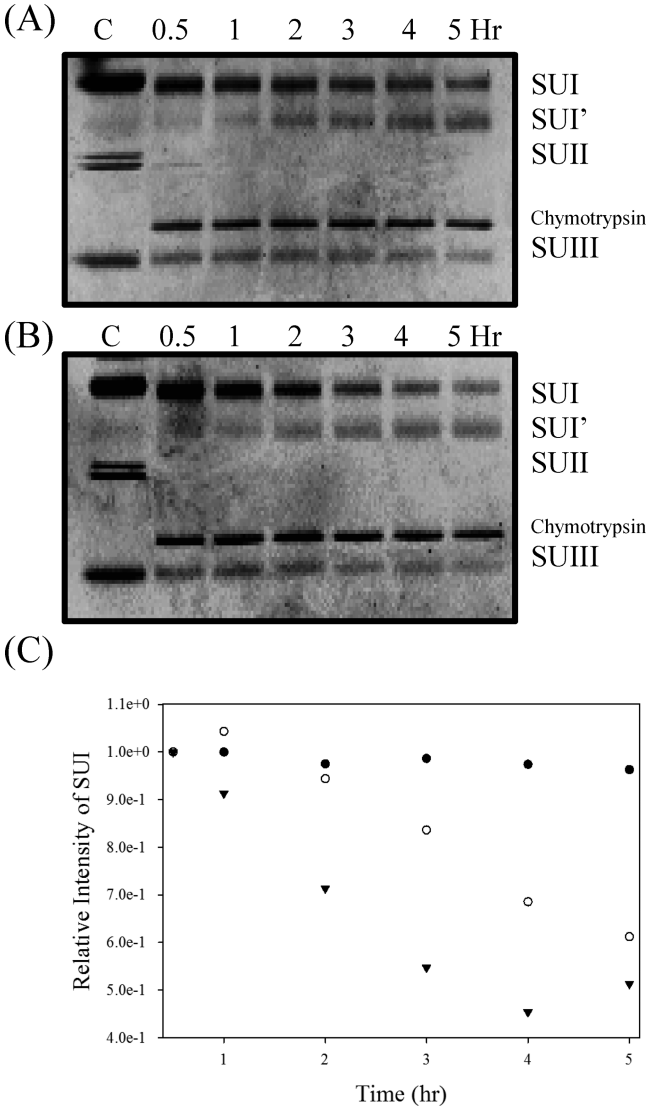

Figure 4. Time dependence of chymotrypsin digestion of WT and delipidated COX. WT and delipidated COX were treated with a 10:1 (w/w) chymotrypsin:COX ratio for various times and quenched with 1 mM PMSF. Five micrograms of COX was loaded into each lane of a SDS–PAGE gel. The time course for WT COX is shown in panel A and that for delipidated COX in panel B, and panel C shows the fractional band intensity of SUI for each time course. Data from untreated control (●), treated WT (○), and delipidated COX (▼) are shown. SUI′ is a chymotrypsin digestion fragment.

decreased over time with new bands appearing and running faster than SUI, and that the delipidated enzyme exhibited an accelerated rate of digestion. This confirms that structural motion or increased flexibility is occurring more rapidly in delipidated COX SUI and that the enzyme exhibits a relaxed, open conformation in the absence of lipids that makes SUI more labile for chymotrypsin digestion.

To confirm that motion in SUIII occurs as a result of the removal of phospholipids, fluorescence anisotropy of WT and delipidated COX was measured using AEDANS as a fluorescent probe linked to SUIII. Figure 5 shows that the specificity of

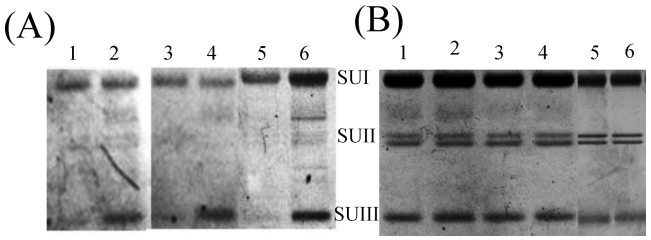

Figure 5. Specificity of binding of AEDANS to SUIII of COX. (A) SDS–PAGE of 5 μg of COX reacted with AEDANS. Fluorescence from AEDANS was observed by excitation under 312 nm light using a Fuji LAS-3000 imager. (B) Coomassie Blue-stained gel. Contents of each gel: lane 1, unlabeled WT; lane 2, AEDANS-labeled WT; lane 3, unlabeled delipidated COX; lane 4, AEDANS-labeled delipidated COX; lane 5, unlabeled SUIII A4C mutant; lane 6, AEDANS labeled A4C mutant.

AEDANS labeling is limited to SUIII in both WT and delipidated COX. The stoichiometry of binding of AEDANS to COX was calculated by absorbance spectroscopy to be 0.5 mol of AEDANS/mol of COX. The polarization of the AEDANS covalently bound to WT displayed an anisotropy higher than that of AEDANS bound to delipidated COX. This translates into a faster rotational rate of the probe in the absence of lipids, supporting an increase in conformational flexibility (Table 3).

Table 3. Fluorescence Anisotropies of Fluorophore-Labeled WT and Delipidated COX

	AEDANS[a]	TFCL[b]
WT	0.22 ± 0.02	0.09 ± 0.001
delipidated	0.17 ± 0.02	0.16 ± 0.001

[a]AEDANS anisotropy measured using an ISS PC1 spectrofluorimeter (λ_{ex} = 336 nm, and λ_{em} = 470 nm). [b]λ_{ex} = 490 nm, and λ_{em} = 505 nm.

Localization of the Lipids in *RBS* COX. To ascertain the role of phospholipids in COX function, FRET was used to map intermolecular distances between a fluorescent CL derivative (TFCL) and AEDANS-labeled SUIII. Table 2 shows that CL stimulates activity in the delipidated COX, and we observed that addition of TFCL results in a level of stimulation of activity similar to that of CL. Thus, in these FRET studies, the concentration of TFCL utilized was under saturating conditions for the high-affinity site of interaction of CL with COX (Figure 2).

The kinetics of the change in FRET efficiency was studied by exciting AEDANS at 336 nm and monitoring the emission of TFCL at 505 nm until the emission reached a steady-state value (Figure 6). FRET in the WT exhibited monophasic kinetics with a rate of 0.016 ± 0.002 s^{-1}, while delipidated COX exhibited biphasic kinetics with rates of 0.104 ± 0.035 and 0.026 ± 0.002 s^{-1}. It is most likely that the fast kinetic phase correlates with the high-affinity CL binding site, which is occupied by other phospholipids in WT and, thus, not observed in WT. The slow kinetic phase in Figure 6 correlates with the low-affinity CL binding site, which occurs in both WT and delipidated COX. The amplitude of the emission is also indicative of TFCL binding at different locations between WT and delipidated COX (Figure 6). This suggests that the TFCL binding site is located in a more hydrophobic environment in delipidated COX, resulting in a higher emission intensity (Figure 6).

DOI: 10.1021/bi5013657
Biochemistry 2015, 54, 1053–1063

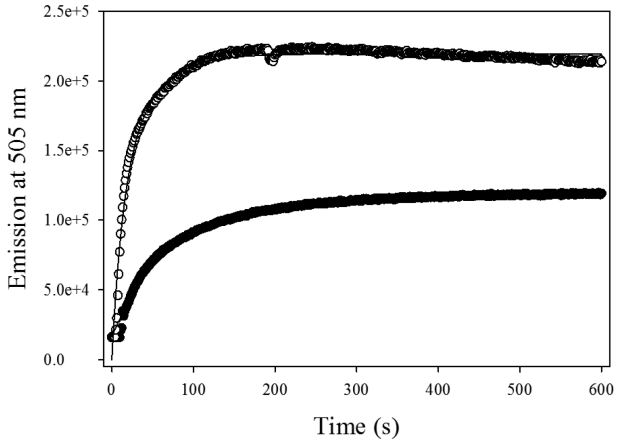

Figure 6. Kinetics of FRET between AEDANS and TopFluor cardiolipin in WT and delipidated COX. Measurements were taken with an ISS PC1 spectrofluorimeter. To a solution of either 0.5 μM WT COX (●) or delipidated COX (○) in 50 mM potassium phosphate (pH 7.4) and 50 μM DM was added 1 μM TFCL. AEDANS was excited at 336 nm, and fluorescence emission was monitored at 505 nm continuously for 600 s with 1 s time intervals. The WT COX data were fit to a single-exponential curve with a rate of 0.016 ± 0.002 s^{-1} and an R^2 of 0.9815, and the delipidated COX data were fit to an exponential curve with two rates of 0.104 ± 0.035 and 0.026 ± 0.002 s^{-1} with an R^2 of 0.9893.

Fluorescence anisotropy measurements (Table 3) provided additional evidence that TFCL binds at separate sites within WT versus delipidated COX. The anisotropy of the TFCL was greater in delipidated COX than in WT COX, indicating that the motion of TFCL when it is bound is more restricted in the delipidated COX. This means that TFCL is most likely interacting with SUIII in the v-shaped cleft as compared to the location at the interface among SUI, SUIII, and SUIV, which is predicted to be a less restricted and more flexible binding site because of its large volume estimated from the crystal structure (see Discussion).

Figure 7A shows the emission spectrum of AEDANS-labeled WT COX and delipidated COX in the absence (solid lines) and presence (dashed lines) of TFCL. Figure 7B shows that in delipidated COX, the AEDANS fluorescence is more efficiently quenched by TFCL, suggesting the proximity to AEDANS. Using these data, the calculated distance between the AEDANS label on SUIII and TFCL is 46.7 ± 1.3 Å in WT (black) and 40.7 ± 2.1 Å in delipidated COX (red) (Figure 7 and Table 4).

In the absence of lipids, TFCL binds at a location closer to the covalently attached AEDANS in SUIII as compared to WT. The distances obtained from the three-dimensional crystal structure (Figure 8A) in comparison to distances measured by FRET (Table 4) predict the location of the high-affinity site in delipidated COX to be in the v-shaped cleft of SUIII. Alternatively, the location of the low-affinity site in WT is predicted to be at the interface between SUI, SUIII, and SUIV (Figure 8B). The distances shown were measured from the predicted linkage site of AEDANS, C143 of SUIII, to conserved residues that form salt bridges with the phosphate groups of the phospholipids.

A mutant form of the enzyme in SUIII (A4C), where all the cysteine residues have been mutated to alanine and A4 in SUIII was mutated to cysteine, was also used in similar FRET studies. The oxidized and reduced heme absorbance spectra of mutant A4C were similar to those of WT, and the mutant exhibited

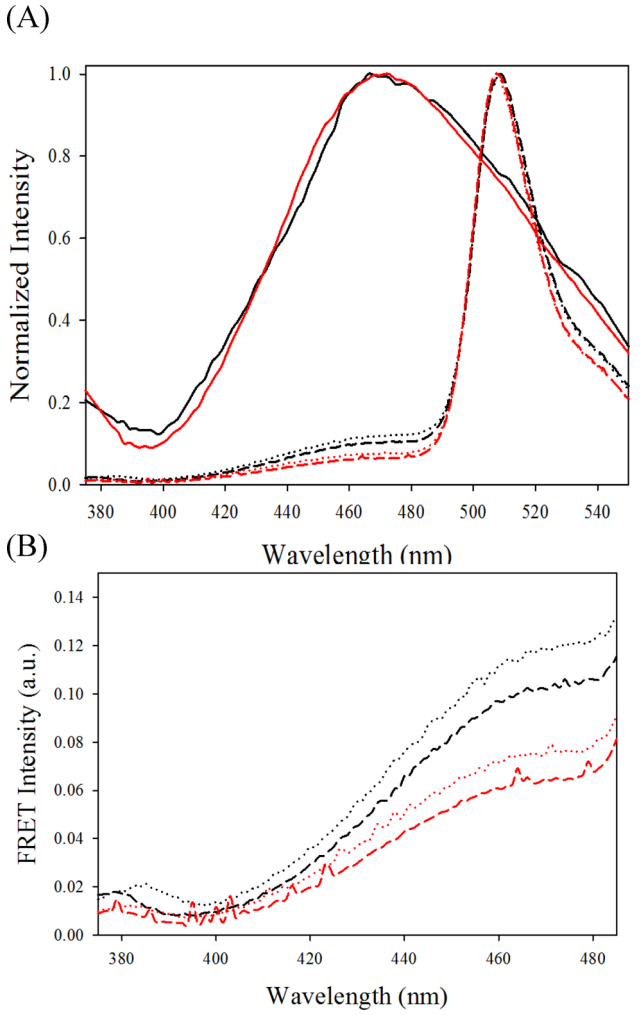

Figure 7. FRET between AEDANS and TFCL in WT and delipidated COX. In panel A, the emission scan of TFCL at 375−550 nm was recorded in the presence of AEDANS-labeled COX upon excitation at 336 nm. Traces were normalized to the maximal intensity to show the difference in emission quenching of the donor. For the calculation of efficiency, the raw data were used. Concentrations of COX and TFCL were 0.5 and 1 μM, respectively, in 50 mM potassium phosphate (pH 7.4) and 50 μM DM. WT COX data are shown in black and delipidated COX data in Red. The emission of AEDANS in the absence of TFCL is shown as solid lines. The quenching of AEDANS emission in the presence of TFCL is shown as dashed lines, and quenching in the presence of TFCL and 7 mM ascorbic acid is shown as dotted lines. In panel B, a magnification of the FRET data from panel A is presented.

WT activity (data not shown).[42] SUIII of the A4C mutant was specifically labeled with AEDANS (Figure 5A,B), and the distance between AEDANS at A4C and TFCL was measured to be 45.9 ± 1.9 Å (data not shown), which agrees with the distance measured in WT. Thus, TFCL presumably binds at the interface between SUI, SUIII, and SUIV in COX with normal levels of endogenous lipids.

Perturbation of Lipid Position in COX with Changes in Redox State at the Active Site in the Presence of Electrons. Previous work using deuterium exchange with mass spectroscopy has shown that *RBS* COX undergoes protein conformational changes during catalytic intermediate formation.[43] We wanted to test if our FRET analysis using AEDANS and TFCL could be used to assess protein conformational

DOI: 10.1021/bi5013657
Biochemistry 2015, 54, 1053−1063

Table 4. Summary of Distances Measured by FRET in WT and Delipidated COX

	WT	delipidated COX
predicted distance in structure[a]	46.2 ± 7.8	40.1 ± 3.2
measured distance from FRET	46.7 ± 1.3	40.7 ± 2.1
FRET distance during steady state[b]	49.8 ± 1.5	44.1 ± 1.7

[a]The distance from the predicted AEDANS binding site on C143 of SUIII and SUIII amino acid residues that interact with lipids was measured using coordinates from Protein Data Bank entry 1M56. The WT distances were measured from AEDANS to amino acid residues that interact with lipids at the interface among SUI, SUIII, and SUIV, while those for delipidated COX were measured to amino acid residues that interact with lipids within the v-shaped cleft in SUIII. [b]Distances measured by FRET between AEDANS and TFCL in the presence of 20 mM ascorbic acid.

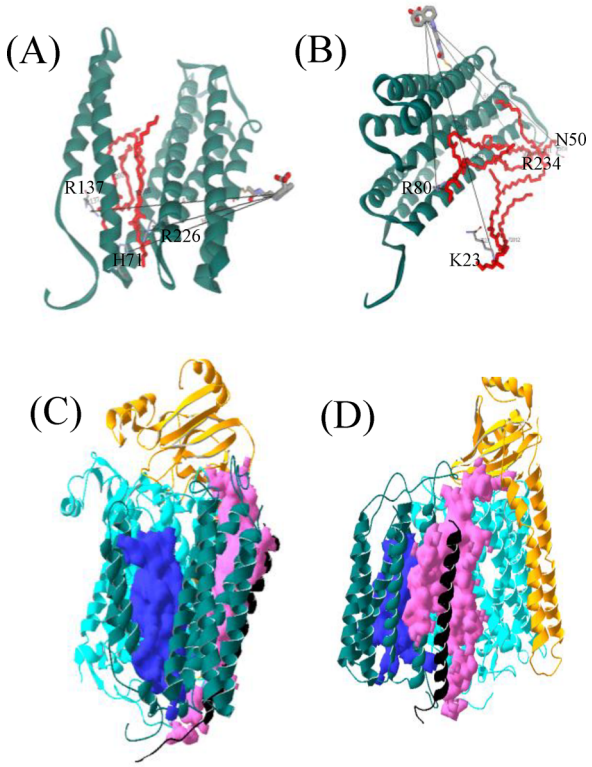

Figure 8. Predicted TFCL interaction site with SUIII of WT and delipidated COX. SPDBV was used to measure distances separating C143 and predicted lipid binding sites. Coordinates from Protein Data Bank entry 1M56 were used.[3] (A) Distance measurements between AEDANS-labeled C143 and residues that interact with lipids in the v-shaped cleft. Distances reported between AEDANS and R137 (SUI) of 41.96 Å, H71 (SUIII) of 36.34 Å, and R226 (SUIII) of 41.96 Å. (B) Distance measurements between AEDANS-labeled C143 and residues that interact with lipids at the interface between SUI, SUIII, and SUIV. Distances listed between AEDANS and R234 (SUII) of 51.58 Å, N50 (SUIV) of 49.07 Å, R80 (SUIII) of 34.57 Å, and K23 (SIV) of 49.53 Å. (C) View of the volume of the v-shaped cleft in SUIII, measured at 2099 Å^3 using SPDBV. (D) View of the interface volume between SUI, SUIII, and SUIV measured at 4379 Å.[3] In panels C and D, SUI is colored turquoise, SUII is colored yellow, SUIII is colored green, SUIV is colored black, and lipids are colored purple and pink.

changes in WT and delipidated *RBS* COX. Previously, bovine heart COX has been reported to exhibit a slow rate of oxygen reduction activity in the presence of ascorbate (<1 s^{-1}).[44] Also, heme *a* has been shown to be reduced by ascorbate.[45] The effect of ascorbate on FRET between AEDANS and TFCL was monitored to determine if any changes in the interaction between the protein and lipid occurred. Cytochrome *c* was omitted from these studies because of its interference with energy transfer between the two chromophores because of its high absorbance in that region of the visible spectrum. Upon addition of ascorbate to WT and delipidated COX, a red shift in the absorbance of the heme in the Soret region occurred, from 425 nm (oxidized) to 430 nm, which is characteristic of heme *a* reduction and limited steady-state turnover activity (Figure 9A,B). The dependence of absorbance at 430 nm on ascorbate

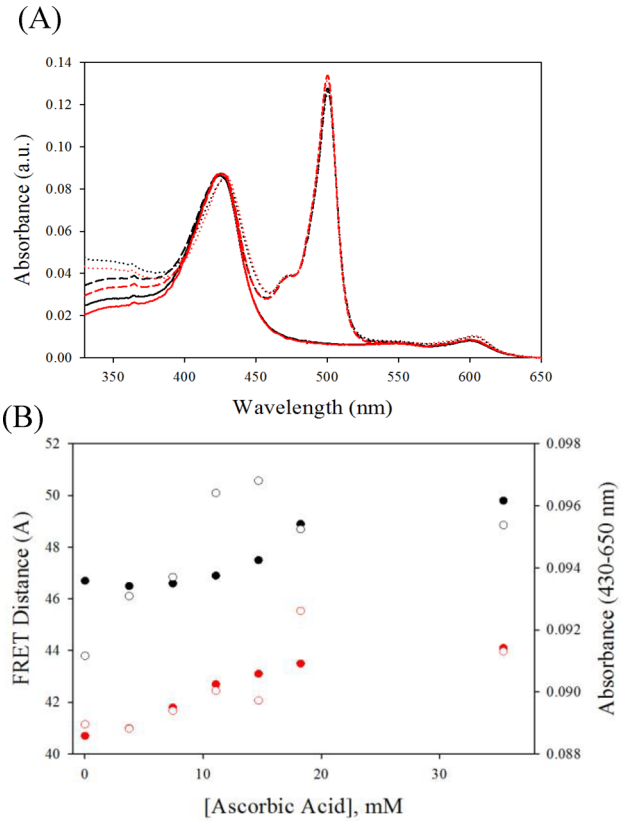

Figure 9. Effect of ascorbic acid on heme *a* absorbance and on FRET. (A) Absorbance changes upon the different treatments. Shown in black are WT data and in red delipidated COX data. The solid line shows data for 0.5 μM COX, the dashed line data for 0.5 μM COX and 1 μM TFCL, and the dotted line data for 0.5 μM COX, 1 μM TFCL, and 7 mM ascorbic acid. The maximum at the Soret region shifts from 425 nm in the oxidized state to 430 nm in the presence of ascorbic acid. (B) The dependence of the absorbance at 430 nm on ascorbic acid concentration for WT (○) and delipidated COX (○, red) is shown using the right axis. The dependence of the distance measured from FRET on ascorbic acid concentration for WT (●) and delipidated COX (●, red) is shown using the left axis.

concentration for WT and delipidated COX is shown in Figure 9B. Similarly, fluorescence emission by AEDANS quenched by TFCL changes upon the addition of ascorbate in a concentration-dependent manner and in a manner independent of inner filter effects (Figure 7A,B). Figure 9B also shows the changes in distance between AEDANS and TFCL measured by FRET (calculated from the data in Figure 7B) in the presence of ascorbate (●). Both the absorbance shift at 430 nm and FRET changes are saturated at ~15 mM ascorbate [Figure 9B (○ and ●, respectively)]. The change in distance between the

DOI: 10.1021/bi5013657
Biochemistry 2015, 54, 1053−1063

fluorophores suggests that electrons present in the complex induce a change in position between the probes (Figure 9B). Upon the addition of ascorbate, the donor (AEDANS) and acceptor (TFCL) distance increases by 3−4 Å, suggesting that TFCL shifts closer to SUI. In contrast, the A4C mutant exhibits a 3−4 Å decrease in the distance between the two fluorophores (data not shown). Our results suggest that the lipids may facilitate a more compact conformation of the enzyme structure during catalytic turnover (see Discussion).

DISCUSSION

Previous work has shown that lipids are retained in the three-dimensional crystalline structures of many integral membrane proteins. COX from both mitochondrial and bacterial sources contains phospholipids intercalated in their structures at conserved lipid binding sites. These putative "structural" lipids serve a role distinctly different from that of boundary lipids, which are freely exchangeable within the membranes. Our experiments addressed the role of the structural lipid in *RBS* COX structure and function.

Effect of Phospholipids on the Interaction between SUI and SUIII. Previous work utilizing mutations within the lipid binding sites in SUIII resulted in a loss of SUIII, suggesting that lipids are necessary for the proper assembly of SUIII with SUI.[10] Alternatively, we have shown that when lipids are extracted from the purified WT, there is little or no loss of SUIII. Thus, incorporation of lipid into the enzyme and lipid depletion of the enzyme are mutually exclusive processes.

Specificity of Phospholipids Required for Reconstitution of the Activity in Delipidated COX. The removal of phospholipids by PLA_2 treatment decreased steady-state electron transfer activity and increased suicide inactivation. The PLA_2 treatment induces a 30−50% inhibition of activity observed as a result of the delipidation, which it not due to the loss of SUIII. The reversibility of this inhibition and suicide inactivation was achieved only when the delipidated enzyme was incubated with CL and long chain fatty acids (Table 2). Upon delipidation of COX, the structure relaxes to a more open conformation, and thus, the addition of long chain fatty acids to the enzyme can help provide the D-channel with additional protons for an increased rate of enzymatic turnover as shown previously.[13,46]

The crystal structure of *RBS* COX shows PE as the predominant phospholipid bound in SUIII; however, PE did not restore the activity of the delipidated COX (Table 2). This was intriguing considering that 40% of the bacterial membrane is composed of PE;[33] however, CL was the most effective phospholipid in stimulating the activity of the delipidated COX. Zhang et al.,[34] using a mutation in the CL synthase in *RBS* in combination with growth on phosphate and phosphate-limited media, showed that in membranes and in purified COX, biosynthesis of negatively charged phospholipids such as PG and sulfolipids is increased to compensate for CL depletion. Although the isolated enzymes retained their activity, the authors provided evidence that biosynthesis of CL is the highest priority for *RBS* with PG as a secondary priority, and then PE and PC as tertiary priorities. They conclude that structural features of CL are more important for both membranes and COX than PC and PE (even though PE is present in the crystal structure).

Additionally, Arias-Cartin et al.[47] suggested that different phases in bacterial growth yield membranes with different phospholipid compositions. *Bacillus subtilis* and *Escherichia coli* both undergo changes in CL composition in their membranes in the exponential and stationary phases of growth, suggesting that some bacteria have flexibility for biosynthesis of lipids during cell growth. We believe that growth conditions and purification protocol may have contributed to the lipid composition of our purified enzyme as compared to the conditions used for crystallization.

Finally, conserved amino acids in the near vicinity of the phospholipids in the crystal structure are basic, such as H10, H71, H231, and H237, which makes the environment more accommodating for a negatively charged phospholipid, i.e., cardiolipin. Our data suggest that cardiolipin can replace the function of PE found in the crystal structure.

The arrangement of helices in SUIII allows lipids to bind within its cleft. SPDBV[48] was used to calculate volumes of putative binding pockets in the structure of SUIII. Panels C and D of Figure 8 show that two major binding pockets were detected; the first is located within the v-shaped cleft with a volume of 2099 $Å^3$, and the second is located at the interface between SUI, SUIII, and SUIV with a volume of 4379 $Å^3$. VEGAA ZZ[49] was used to estimate the van der Waals volume of CL to be 1716 $Å^3$. Accordingly, one molecule of CL is capable of fitting within the volume of the v-shaped cleft in SUIII. Additionally, the volume of the binding pocket within the interface between SUI, SUIII, and SUIV is approximately twice the volume of CL. Thus, we have measured the space occupied by PE in the crystal structure, and we find that CL fits perfectly in both proposed sites.

Upon the addition of CL, delipidated COX exhibits biphasic steady-state kinetics in activity. The high-affinity site is presumably located within the well-defined binding pocket in the v-shaped cleft in SUIII, which is less accessible to solvent. This site is occupied in WT COX and vacant in delipidated COX. Alternatively, the low-affinity site for CL is likely to be at the interface between SUI, SUIII, and SUIV. The measured volume at the interface is capable of accommodating two molecules of CL; however, these possible sites may have the same properties and affinities. Thus, our data cannot exclude this possibility.

Steady-State Kinetics of Interaction of Cytochrome *c* with COX. Previous work on bovine COX showed that cytochrome *c* has two distinct steady-state kinetic and binding sites.[40] The high-affinity binding site for cytochrome *c* is located on SUII, while the low-affinity site is facilitated through lipids.[40] Vik et al. showed that, in the absence of lipids, bovine heart COX loses the low-affinity site, and the addition of exogenous CL reconstitutes the site.[11] COX purified from *RBS* exhibits biphasic kinetic properties similar to those of bovine heart COX.[25] In delipidated COX, we showed that the low-affinity kinetic site is lost but can be reconstituted by the addition of CL (Figure 3). Upon the addition of CL, activity is increased, suggesting that CL in the low-affinity kinetic site plays an important role in steady-state turnover activity. The double negative charge carried by CL has been proposed to assist in the electrostatic interactions that could tether cytochrome *c* to the enzyme.[40]

Lipids Regulate Structural Flexibility. Phospholipids have been proposed to serve a facilitative role in the assembly of the enzyme into an optimal three-dimensional conformation.[12] We tested this hypothesis using two different methods. Limited proteolysis with chymotrypsin demonstrated that SUI of the delipidated COX exhibited a rate of digestion that was faster than that of WT. This suggests that SUI of the

DOI: 10.1021/bi5013657
Biochemistry 2015, 54, 1053−1063

delipidated enzyme exists in a more open conformation or has an increased degree of freedom of motion in its structure. Alternatively, it could be that the removal of the lipids simply exposes the new cleavage sites for chymotrypsin; in our view, this is improbable because of the similar size of the SUI-digested band on SDS−PAGE in both enzyme forms. We have determined that chymotrypsin cleaves SUI after the six N-terminal amino acids and also 44 amino acids from the C-terminus.[41]

Thus, it is likely that the delipidated enzyme is in a more open conformation. The second method for providing evidence of increased flexibility in SUIII being translated to SUI is the increased degree of rotational freedom of AEDANS-labeled SUIII in the delipidated enzyme (Table 3). This increase results in more flexibility in COX in the absence of lipids, which is translated to SUI. Alternatively, our results could also be interpreted as an increase in localized SUIII flexibility in the region of the AEDANS fluorophore.

Differential Cardiolipin Binding in WT and Delipidated COX. FRET measurements showed that TFCL binds to the delipidated COX at a different location compared to that of WT (Figure 7A). Measurements by FRET show that the distance separating the pair of fluorophores (AEDANS and TFCL) is 46.7 ± 1.3 Å for the WT compared to 40.7 ± 2.1 Å for delipidated COX, suggesting that TFCL binds at different locations in WT and delipidated COX. The increased distance from AEDANS in SUIII to TFCL in WT reinforces the idea that TFCL is binding at the interface between SUI, SUIII, and SIV. The maximal emission intensity also indicates that the environment at which TFCL binds to the delipidated COX is more hydrophobic than that of WT COX (Figure 6).

Localization of the Cardiolipin Binding Site. The crystal structure of COX was used to locate possible sites where the binding of TFCL would occur in WT and delipidated COX. Figure 8A shows distances reported between Cys143 (predicted linkage site of AEDANS) and several residues of SUIII where phospholipids may interact. Two of the phospholipids in the crystal structure are located within the v-shaped cleft. A distance of 12.6 Å separates the phosphate groups from both lipids, and at half the distance, there is a highly conserved histidine residue (H71), where the imidazole ring is oriented toward the middle of the distance between the lipids. Alternatively, the distance separating the two phosphate groups of CL is ∼8 Å, which can vary depending on the structure.[50] Accordingly, it is hypothesized that H71, which has not been mutated to date, is a possible site to which the hydroxyl group of CL could interact at the v-shaped cleft.

The measured distances (Figure 8 and Table 4) show that the lipids at the interface between SUI, SUIII, and SUIV are located farther from the AEDANS moiety when compared to those at the v-shaped cleft of SUIII. The distances measured from FRET correlate with the proposed location of TFCL in both WT and delipidated COX. It is proposed that TFCL binds at the interface in WT and at the v-shaped cleft of SUIII in delipidated COX (Table 4).

Detected Motion in SUIII upon the Addition of Electrons. Upon transfer of electrons from ascorbate, the distance between TFCL and AEDANS in both WT and delipidated COX increased 3−4 Å. This conformational change is likely directed toward SUI, and we propose that it could assist with the delivery of oxygen to the active site, as previously proposed.[6] These structural changes are supported by recent neutron scattering studies that show that bovine heart COX has a structure in liposomes more condensed than that of the crystal structure.[51]

Lipids are proposed to form the oxygen pathway because of the higher partition coefficient of oxygen in lipids.[6] Specifically, the lipids regulate motion at the active site via long-range interactions to keep the active site intact and eliminate damaging side reactions, which can lead to suicide inactivation. Thus, as a consequence of delipidation, regulation of motion at the active site is absent, and consequently, the enzyme undergoes turnover-induced suicide inactivation, with Cu_B ultimately being lost.

FRET data of the A4C mutant are possibly less reliable because the N-terminus of SUIII, which contains the proposed proton-collecting antenna, may have motion associated with electron transfer from ascorbate.[9] Nonetheless, the data show that TFCL and AEDANS at A4C move closer to each other in the presence of electrons. We propose that upon a change in the redox state of COX, the bound phospholipids move closer to SUI and condense the structure. This creates a more rigid structure allowing for better control over the structural motion of the active site. Additionally, this could assist in oxygen delivery and allow for protons to be transferred through the D-channel more efficiently. Our hypothesis is supported by studies showing that the N-terminal peptide of SUIII (2−26) has a rate of deuterium exchange higher than those of other SUIII regions, which increases significantly for the F intermediates.[43]

In conclusion, this study proposes a novel mechanism by which phospholipids could regulate the integrity of the structure of COX, especially at the binuclear center. It is proposed that the lipids condense the structure horizontally along the membrane to allow for efficient delivery of oxygen to the active site and vertically to allow for efficient delivery of protons to the active site. Finally, the lipids may control the flexibility at the active site to modulate structural movement, thus allowing for efficient oxygen binding and efficient electron transfer activity.

This study suggests that in the absence of phospholipids, the catalytic core of COX becomes more flexible. Thus, the lipids are necessary to regulate the structural motion near the active site to increase the rate of electron transfer activity and prevent suicide inactivation.

AUTHOR INFORMATION

Corresponding Author

*E-mail: lawrence.prochaska@wright.edu. Phone: (937) 775-2551.

Present Addresses

[†]K.S.A.: Department of Therapeutic Radiology, School of Medicine at Yale University, New Haven, CT 06520-8040.

[‡]T.C.: Max F. Perutz Laboratories, Structural and Computational Biology, Vienna, Austria.

Funding

Support was provided by the Wright State University Foundation in memory of Henry and Emily Webb and the Boonshoft School of Medicine at Wright State University. K.S.A. was supported by the Biomedical Sciences Ph.D. program at Wright State University.

Notes

The authors declare no competing financial interest.

DOI: 10.1021/bi5013657
Biochemistry 2015, 54, 1053−1063

■ ACKNOWLEDGMENTS

We thank Dr. Chad Hammerschmidt and Alison Agather for their assistance with ICP-MS. We also thank Dr. Heather Hostetler and Dr. Gerald Alter for the useful discussions and Dr. Christine Pokalsky for editing the manuscript.

■ ABBREVIATIONS

CL, cardiolipin; COX, cytochrome *c* oxidase; DM, *n*-dodecyl β-D-maltoside; IAEDANS, 5-({[(2-iodoacetyl)amino]ethyl}-amino)naphthalene-1-sulfonic acid; ICP-MS, inductively coupled plasma mass spectrometry; NTA, nitrilotriacetic acid; PC, phosphatidylcholine; PE, phosphatidylethanolamine; PG, phosphatidylglycerol; PMSF, phenylmethanesulfonyl fluoride; *RBS*, *R. sphaeroides*; SDS−PAGE, sodium dodecyl sulfate−polyacrylamide gel electrophoresis; SPDBV, Swiss Protein Data Bank Viewer; SUI, subunit I; SUII, subunit II; SUIII, subunit III; TFCL, 1,1′,2,2′-tetraoleoyl cardiolipin [4-(dipyrromethene-boron difluoride) butanoyl]; TMPD, tetramethylphenylenediamine; WT, wild type.

■ ADDITIONAL NOTE

[a]Amino acid residues are numbered according to the cytochrome *c* oxidase sequence from *R. sphaeroides* unless otherwise noted.

■ REFERENCES

(1) Wikstrom, M. K. (1977) Proton pump coupled to cytochrome *c* oxidase in mitochondria. *Nature 266*, 271−273.
(2) Michel, H., Behr, J., Harrenga, A., and Kannt, A. (1998) Cytochrome *c* oxidase: Structure and spectroscopy. *Annu. Rev. Biophys. Biomol. Struct. 27*, 329−356.
(3) Svensson-Ek, M., Abramson, J., Larsson, G., Tornroth, S., Brzezinski, P., and Iwata, S. (2002) The X-ray crystal structures of wild-type and EQ(I-286) mutant cytochrome *c* oxidases from *Rhodobacter sphaeroides*. *J. Mol. Biol. 321*, 329−339.
(4) Prochaska, L. J., and Reynolds, K. A. (1986) Characterization of electron-transfer and proton-translocation activities in bovine heart mitochondrial cytochrome *c* oxidase deficient in subunit III. *Biochemistry 25*, 781−787.
(5) Prochaska, L. J., and Fink, P. S. (1987) On the role of subunit III in proton translocation in cytochrome *c* oxidase. *J. Bioenerg. Biomembr. 19*, 143−166.
(6) Hofacker, I., and Schulten, K. (1998) Oxygen and proton pathways in cytochrome *c* oxidase. *Proteins 30*, 100−107.
(7) Gilderson, G., Salomonsson, L., Aagaard, A., Gray, J., Brzezinski, P., and Hosler, J. (2003) Subunit III of cytochrome c oxidase of *Rhodobacter sphaeroides* is required to maintain rapid proton uptake through the D pathway at physiologic pH. *Biochemistry 42*, 7400−7409.
(8) Mills, D. A., Tan, Z., Ferguson-Miller, S., and Hosler, J. (2003) A role for subunit III in proton uptake into the D pathway and a possible proton exit pathway in *Rhodobacter sphaeroides* cytochrome *c* oxidase. *Biochemistry 42*, 7410−7417.
(9) Alnajjar, K. S., Hosler, J., and Prochaska, L. (2014) Role of the N-terminus of subunit III in proton uptake in cytochrome *c* oxidase of *Rhodobacter sphaeroides*. *Biochemistry 53*, 496−504.
(10) Varanasi, L., Mills, D., Murphree, A., Gray, J., Purser, C., Baker, R., and Hosler, J. (2006) Altering conserved lipid binding sites in cytochrome c oxidase of *Rhodobacter sphaeroides* perturbs the interaction between subunits I and III and promotes suicide inactivation of the enzyme. *Biochemistry 45*, 14896−14907.
(11) Vik, S. B., Georgevich, G., and Capaldi, R. A. (1981) Diphosphatidylglycerol is required for optimal activity of beef heart cytochrome *c* oxidase. *Proc. Natl. Acad. Sci. U.S.A. 78*, 1456−1460.
(12) Sedlak, E., and Robinson, N. C. (1999) Phospholipase A_2 digestion of cardiolipin bound to bovine cytochrome *c* oxidase alters both activity and quaternary structure. *Biochemistry 38*, 14966−14972.
(13) Varanasi, L., and Hosler, J. (2011) Alternative initial proton acceptors for the D pathway of *Rhodobacter sphaeroides* cytochrome *c* oxidase. *Biochemistry 50*, 2820−2828.
(14) Tsukihara, T., Aoyama, H., Yamashita, E., Tomizaki, T., Yamaguchi, H., Shinzawa-Itoh, K., Nakashima, R., Yaono, R., and Yoshikawa, S. (1996) The whole structure of the 13-subunit oxidized cytochrome *c* oxidase at 2.8 Å. *Science 272*, 1136−1144.
(15) Zhen, Y., Hoganson, C. W., Babcock, G. T., and Ferguson-Miller, S. (1999) Definition of the interaction domain for cytochrome *c* on cytochrome *c* oxidase. I. Biochemical, spectral, and kinetic characterization of surface mutants in subunit II of *Rhodobacter sphaeroides* cytochrome aa_3. *J. Biol. Chem. 274*, 38032−38041.
(16) Schagger, H., Hagen, T., Roth, B., Brandt, U., Link, T. A., and von Jagow, G. (1990) Phospholipid specificity of bovine heart bc_1 complex. *Eur. J. Biochem. 190*, 123−130.
(17) Fry, M., and Green, D. E. (1981) Cardiolipin requirement for electron transfer in complex I and III of the mitochondrial respiratory chain. *J. Biol. Chem. 256*, 1874−1880.
(18) Gomez, B., Jr., and Robinson, N. C. (1999) Phospholipase digestion of bound cardiolipin reversibly inactivates bovine cytochrome bc_1. *Biochemistry 38*, 9031−9038.
(19) Zhen, Y., Qian, J., Follmann, K., Hayward, T., Nilsson, T., Dahn, M., Hilmi, Y., Hamer, A. G., Hosler, J. P., and Ferguson-Miller, S. (1998) Overexpression and purification of cytochrome *c* oxidase from *Rhodobacter sphaeroides*. *Protein Expression Purif. 13*, 326−336.
(20) Junemann, S., Meunier, B., Gennis, R. B., and Rich, P. R. (1997) Effects of mutation of the conserved lysine-362 in cytochrome *c* oxidase from *Rhodobacter sphaeroides*. *Biochemistry 36*, 14456−14464.
(21) Bratton, M. R., Pressler, M. A., and Hosler, J. P. (1999) Suicide inactivation of cytochrome *c* oxidase: Catalytic turnover in the absence of subunit III alters the active site. *Biochemistry 38*, 16236−16245.
(22) Sedlak, E., Panda, M., Dale, M. P., Weintraub, S. T., and Robinson, N. C. (2006) Photolabeling of cardiolipin binding subunits within bovine heart cytochrome *c* oxidase. *Biochemistry 45*, 746−754.
(23) Weiss, H., and Juchs, B. (1978) Isolation of a multiprotein complex containing cytochrome *b* and c_1 from *Neurospora crassa* mitochondria by affinity chromatography on immobilized cytochrome *c*. Difference in the binding between ferricytochrome *c* and ferrocytochrome *c* to the multiprotein complex. *Eur. J. Biochem. 88*, 17−28.
(24) Fuller, S. D., Darley-Usmar, V. M., and Capaldi, R. A. (1981) Covalent complex between yeast cytochrome *c* and beef heart cytochrome *c* oxidase which is active in electron transfer. *Biochemistry 20*, 7046−7053.
(25) Hiser, C., Mills, D. A., Schall, M., and Ferguson-Miller, S. (2001) C-terminal truncation and histidine-tagging of cytochrome *c* oxidase subunit II reveals the native processing site, shows involvement of the C-terminus in cytochrome *c* binding, and improves the assay for proton pumping. *Biochemistry 40*, 1606−1615.
(26) Hall, J., Moubarak, A., O'Brien, P., Pan, L. P., Cho, I., and Millett, F. (1988) Topological studies of monomeric and dimeric cytochrome *c* oxidase and identification of the copper A site using a fluorescence probe. *J. Biol. Chem. 263*, 8142−8149.
(27) Hudson, E. N., and Weber, G. (1973) Synthesis and characterization of two fluorescent sulfhydryl reagents. *Biochemistry 12*, 4154−4161.
(28) Strop, P., and Brunger, A. T. (2005) Refractive index-based determination of detergent concentration and its application to the study of membrane proteins. *Protein Sci. 14*, 2207−2211.
(29) Johnson, I. D., Kang, H. C., and Haugland, R. P. (1991) Fluorescent membrane probes incorporating dipyrromethene-boron difluoride fluorophores. *Anal. Biochem. 198*, 228−237.
(30) Wu, P., and Brand, L. (1994) Resonance energy transfer: Methods and applications. *Anal. Biochem. 218*, 1−13.

DOI: 10.1021/bi5013657
Biochemistry 2015, 54, 1053−1063

(31) Larsson, T., Wedborg, M., and Turner, D. (2007) Correction of inner-filter effect in fluorescence excitation-emission matrix spectrometry using Raman scatter. *Anal. Chim. Acta 583*, 357−363.
(32) Yu, C., Yu, L., and King, T. E. (1975) Studies on cytochrome oxidase. Interactions of the cytochrome oxidase protein with phospholipids and cytochrome *c*. *J. Biol. Chem. 250*, 1383−1392.
(33) Ingolia, T. D., and Koshland, D. E., Jr. (1978) The role of calcium in fusion of artificial vesicles. *J. Biol. Chem. 253*, 3821−3829.
(34) Zhang, X., Tamot, B., Hiser, C., Reid, G. E., Benning, C., and Ferguson-Miller, S. (2011) Cardiolipin deficiency in *Rhodobacter sphaeroides* alters the lipid profile of membranes and of crystallized cytochrome oxidase, but structure and function are maintained. *Biochemistry 50*, 3879−3890.
(35) Marinetti, G. V., and Cattieu, K. (1981) Lipid analysis of cells and chromatophores of *Rhodopseudomonas sphaeroides*. *Chem. Phys. Lipids 28*, 241−251.
(36) Yeates, T. O., Komiya, H., Rees, D. C., Allen, J. P., and Feher, G. (1987) Structure of the reaction center from *Rhodobacter sphaeroides* R-26: Membrane-protein interactions. *Proc. Natl. Acad. Sci. U.S.A. 84*, 6438−6442.
(37) Robinson, N. C. (1982) The specificity and affinity of phospholipids for cytochrome *c* oxidase. *Biophys. J. 37*, 65−66.
(38) Robinson, N. C., Zborowski, J., and Talbert, L. H. (1990) Cardiolipin-depleted bovine heart cytochrome *c* oxidase: Binding stoichiometry and affinity for cardiolipin derivatives. *Biochemistry 29*, 8962−8969.
(39) Hosler, J. P., Fetter, J., Tecklenburg, M. M., Espe, M., Lerma, C., and Ferguson-Miller, S. (1992) Cytochrome aa_3 of *Rhodobacter sphaeroides* as a model for mitochondrial cytochrome c oxidase. Purification, kinetics, proton pumping, and spectral analysis. *J. Biol. Chem. 267*, 24264−24272.
(40) Bisson, R., Jacobs, B., and Capaldi, R. A. (1980) Binding of arylazidocytochrome *c* derivatives to beef heart cytochrome *c* oxidase: Cross-linking in the high- and low-affinity binding sites. *Biochemistry 19*, 4173−4178.
(41) Geyer, R. R. (2007) Investigating the role of subunit III in the structure and function of *Rhodobacter sphaeroides* cytochrome c oxidase. Ph.D. Thesis, Wright State University.
(42) Cvetkov, T. (2010) Cytochrome c oxidase from *Rhodobacter sphaeroides*: Oligomeric structure in the phospholipid bilayer and the structural and functional effects of a c-terminal truncation in subunit III. Ph.D. Thesis, Wright State University.
(43) Busenlehner, L. S., Salomonsson, L., Brzezinski, P., and Armstrong, R. N. (2006) Mapping protein dynamics in catalytic intermediates of the redox-driven proton pump cytochrome *c* oxidase. *Proc. Natl. Acad. Sci. U.S.A. 103*, 15398−15403.
(44) Ozawa, T., Takahashi, Y., Malviya, A. N., and Yagi, K. (1974) Reactivity of cytochrome oxidase with ascorbate. *Biochem. Biophys. Res. Commun. 61*, 651−656.
(45) Margoliash, E., Ferguson-Miller, S., Tulloss, J., Kang, C. H., Feinberg, B. A., Brautigan, D. L., and Morrison, M. (1973) Separate intramolecular pathways for reduction and oxidation of cytochrome *c* in electron transport chain reactions. *Proc. Natl. Acad. Sci. U.S.A. 70*, 3245−3249.
(46) Adelroth, P., and Hosler, J. (2006) Surface proton donors for the D-pathway of cytochrome *c* oxidase in the absence of subunit III. *Biochemistry 45*, 8308−8318.
(47) Arias-Cartin, R., Grimaldi, S., Arnoux, P., Guigliarelli, B., and Magalon, A. (2012) Cardiolipin binding in bacterial respiratory complexes: Structural and functional implications. *Biochim. Biophys. Acta 1817*, 1937−1949.
(48) Guex, N., and Peitsch, M. C. (1997) SWISS-MODEL and the Swiss-PdbViewer: An environment for comparative protein modeling. *Electrophoresis 18*, 2714−2723.
(49) Pedretti, A., Villa, L., and Vistoli, G. (2002) VEGA: A versatile program to convert, handle and visualize molecular structure on Windows-based PCs. *J. Mol. Graphics Modell. 21*, 47−49.
(50) Kljashtorny, V. G., Fufina, T. Y., Vasilieva, L. G., and Gabdulkhakov, A. G. (2014) Molecular dynamic studies of reaction centers mutants from *Rhodobacter sphaeroides* and his mutant form L(M196)H+H(M202)L. *Crystallogr. Rep. 59*, 536−541.
(51) Rubinson, K. A., Pokalsky, C., Krueger, S., and Prochaska, L. J. (2013) Structure determination of functional membrane proteins using small-angle neutron scattering (sans) with small, mixed-lipid liposomes: Native beef heart mitochondrial cytochrome *c* oxidase forms dimers. *Protein J. 32*, 27−38.

DOI: 10.1021/bi5013657
Biochemistry 2015, 54, 1053−1063